Electrochemistry Communications 30 (2013) 21–25

Contents lists available at SciVerse ScienceDirect

Electrochemistry Communications

journal homepage: www.elsevier.com/locate/elecom

Ti and Sn co-doped anodic α-Fe_2O_3 films for efficient water splitting

Lei Wang, Chong-Yong Lee, Patrik Schmuki *

Department of Materials Science and Engineering, University of Erlangen-Nuremberg, Martensstrasse 7, D-91058 Erlangen, Germany

ARTICLE INFO

Article history:
Received 15 December 2012
Received in revised form 15 January 2013
Accepted 15 January 2013
Available online 27 January 2013

Keywords:
α-Fe_2O_3
Ti loading
Water splitting
Photocurrent

ABSTRACT

Hematite (α-Fe_2O_3) films were produced by anodic FeOOH deposition on FTO, followed by $TiCl_4$ decoration and an appropriate heat treatment. Optimizing the amount of Ti addition (1.5 μL cm^{-2} of 0.2 M $TiCl_4$) and annealing to 600 °C/750 °C allows to reach 1.4 mA cm^{-2} at 1.23 V (*vs.* RHE) with a maximum photocurrent of 3.1 mA cm^{-2} at 1.8 V (*vs.* RHE) in 1 M KOH under AM 1.5 (100 mW cm^{-2}) simulated solar illumination. This comparably high photoresponse can be attributed to a combined Ti/Sn effect, the latter causing thermal Sn doping from the FTO. Photocurrent transients show that the main combined influence of Ti addition/Sn doping is a strong suppression of charge carrier recombination. This may be attributed to electronic effects but also to a different morphology observed for Ti treated samples. The work shows that simple anodic nanoporous films have a high potential for optimization towards highly efficient hematite based photoelectrodes.

1. Introduction

Since the first reports on photoelectrochemical (PEC) water splitting using a TiO_2 photoelectrode, a high number of other semiconductor materials have been investigated and developed with the ultimate goal to directly convert solar energy into clean and renewable hydrogen fuel [1–5]. Considerable efforts have been directed to using photoanodes of hematite (α-Fe_2O_3) due to its suitable band gap for visible light absorption (≈2.2 eV), its photocorrosion stability, but also due to its abundance and environmental compatibility. In principle, α-Fe_2O_3 has a valence band edge position that allows for an unbiased oxidation of water to oxygen without application of an external bias. However, the PEC activity of α-Fe_2O_3 is limited by several factors, most importantly a short hole diffusion length and a poor oxygen evolution reaction kinetics [4].

Work to improve the electronic properties of iron oxide dates back more than 50 years. Morin [6,7] studied the conduction mechanism in oxides which have partially filled d levels and he attempted to add impurities to increase conductivity. Doping of α-Fe_2O_3, including Si [8,9], Ti [6,10–14], Pt [15,16], Mo [17], Cr [17], and Sn [18,19], has been extensively investigated to yield improved PEC performance. The performance improvement is ascribed to the enhanced conductivity due to the increased donor concentration and catalytic effect, namely a promoted charge-transfer process of photogenerated electrons and holes at the photoanode/electrolyte interface. Highest performance hematite layers meanwhile reach >3 mA cm^{-2} (under AM 1.5 illumination) at elevated applied voltages; usually they are produced by sophisticated (vacuum) or multistep processes [5,14]. Own previous work [20,21] has been based on a simple and cheap anodic α-Fe_2O_3 deposition technique [22] that we optimized towards layer thickness and annealing temperature in view of morphology and solar light water splitting efficiency – we showed that by this trivial approach, remarkable water splitting efficiencies can be reached. In the present work, we explore the effect of Ti impregnation and annealing, i.e. an approach that avoids the use of specialized equipment and metal-organic precursors.

2. Experimental

In order to fabricate FeOOH layers, anodic electrodeposition was carried out according to previous work [20,21] to prepare FeOOH layers of a thickness of ~200 nm (1.95 cm^2 of surface area). As substrate we used fluorine-doped tin oxide glass (FTO-TCO22-15, Solaronix). Before deposition, the FTO glass was washed with acetone, ethanol, and then deionized water. The Ti doping was carried out by pipetting $TiCl_4$ onto the as-prepared FeOOH films. A series of Ti doped α-Fe_2O_3 films was obtained using various amounts of $TiCl_4$ [(0.26 (of 0.02 M $TiCl_4$)), or 0.5, 1.5, 2.6, 5.1, and 10.3 μL cm^{-2} of 0.2 M $TiCl_4$ solutions]. Then the films were annealed in air at 600 °C for 2 h, and then further annealed at 750 °C for an additional 20 min. The second annealing induced substantial Sn diffusion from the FTO glass [18], while still sufficient conductivity of the FTO was provided (as received: 15 ohm/square; after 600 °C: ~20 ohm/square; after 600 °C/750 °C: ~26 ohm/square).

The photoelectrochemical experiments were carried out in three-electrode configuration under simulated AM 1.5 (100 mW cm^{-2}) illumination provided by a solar simulator (300 W Xe with optical filter, Solarlight; RT) in 1 M KOH solution using Ag/AgCl (3 M KCl) as the reference electrode, and a platinum foil as the counter electrode. Photocurrent *vs.* voltage (*I–V*) characteristics and photocurrent spectra were recorded as previously reported [20,21].

* Corresponding author. Tel.: +49 9131 85 275 75; fax: +49 9131 85 275 82.
E-mail address: schmuki@ww.uni-erlangen.de (P. Schmuki).

1388-2481/$ – see front matter © 2013 Elsevier B.V. All rights reserved.
http://dx.doi.org/10.1016/j.elecom.2013.01.013

X-ray diffraction (X'pert Philips MPD with a Panalytical X'celerator detector, Germany) was carried out using graphite monochromized Cu Kα radiation (Wavelength 1.54056 Å). Chemical characterization was carried out by X-ray photoelectron spectroscopy (PHI 5600, spectrometer, USA) using AlKα monochromatized radiation. Time of flight secondary ion mass spectrometry (TOF-SIMS) negative depth profiles were recorded on an Ion-ToF ToF-SIMSS instrument operating in dual beam mode. A pulsed 25 keV Bi^+ liguid-5 metal ion beam bunched down to <0.1 ns was used for spectra generation and a 2 keV Cs^+ ion beam for sputter-removal of the samples (scan rate 0.3 nm s^{-1}). A field-emission scanning electrode microscope (Hitachi FE-SEM S4800, Japan) was used for the morphological characterization of the electrodes.

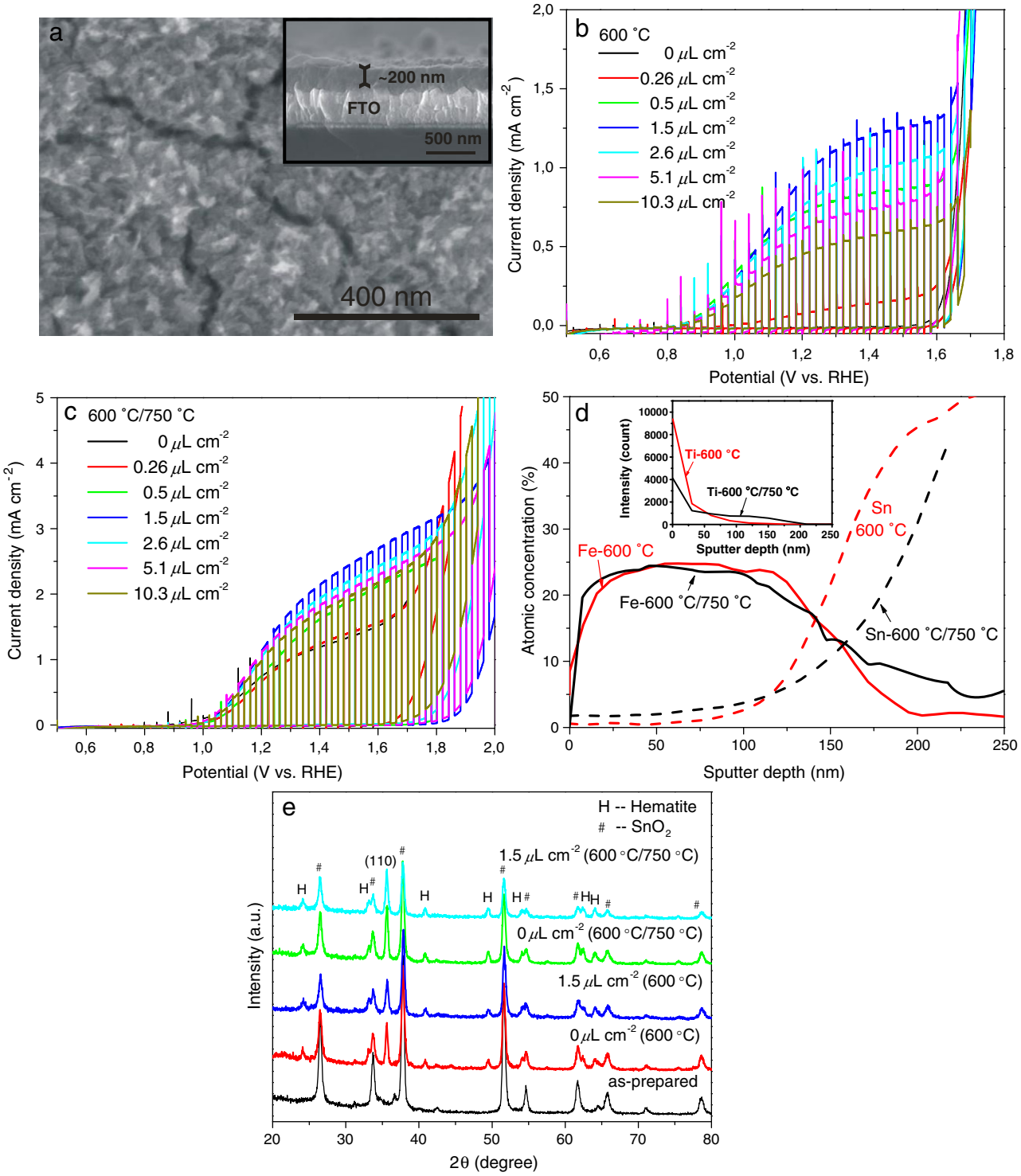

Fig. 1. (a) SEM top view and cross-section of the as-prepared FeOOH film; (b,c) current-potential characteristics with chopped light α-Fe_2O_3/FTO electrodes doped with various amounts of Ti (0.2 M $TiCl_4$) and annealed at (b) 600 °C and (c) 600 °C/750 °C, respectively. *Conditions*: 1 M KOH solution (pH 13.6), 2 mV s^{-1} scan rate. Photocurrent corresponds to AM 1.5 100 mW cm^{-2} simulated sunlight; (d) XPS Fe and Sn depth profiles of 2.6 μL cm^{-2} Ti (0.2 M $TiCl_4$) doped α-Fe_2O_3/FTO electrodes annealed at 600 °C and 600 °C/750 °C (inset of TOF-SIMS Ti depth profiles); (e) XRD patterns of Ti doped α-Fe_2O_3/FTO electrodes annealed at 600 °C and 600 °C/750 °C.

3. Results and discussion

In order to investigate key parameters for Ti-loading we carried out some screening experiments using a ~200 nm thick anodic iron oxide layer on FTO (prepared as in literature [20–22]) (Fig. 1a). Based on our previous work we selected two annealing conditions: 600 °C (where typically full conversion of the anodic deposit layer to hematite can be achieved), and 750 °C where not only annealing but also significant Sn-diffusion (doping) from the FTO substrate into the α-Fe_2O_3 structure can be found [20]. Fig. 1b shows the PEC water splitting results for different amount of Ti doped electrodes after annealing at 600 °C. Consistent with earlier results at 550 °C, the Ti-free sample annealed at 600 °C for 2 h shows a negligible response (<0.02 mA cm^{-2} at 1.23 V (*vs.* RHE)), almost indistinguishable from the dark current. However, significant photocurrents are measured for samples after Ti loading. The photoresponse increases dramatically as the dosing of Ti is increased from 0.26 μL cm^{-2} to 1.5 μL cm^{-2}, and gradually decreased for doses of 2.6 μL cm^{-2} and higher. The optimum dosed Ti electrode with 1.5 μL cm^{-2} shows a plateau in the potential range from 1.2 V (*vs.* RHE) to 1.6 V (*vs.* RHE); in our case with a photocurrent

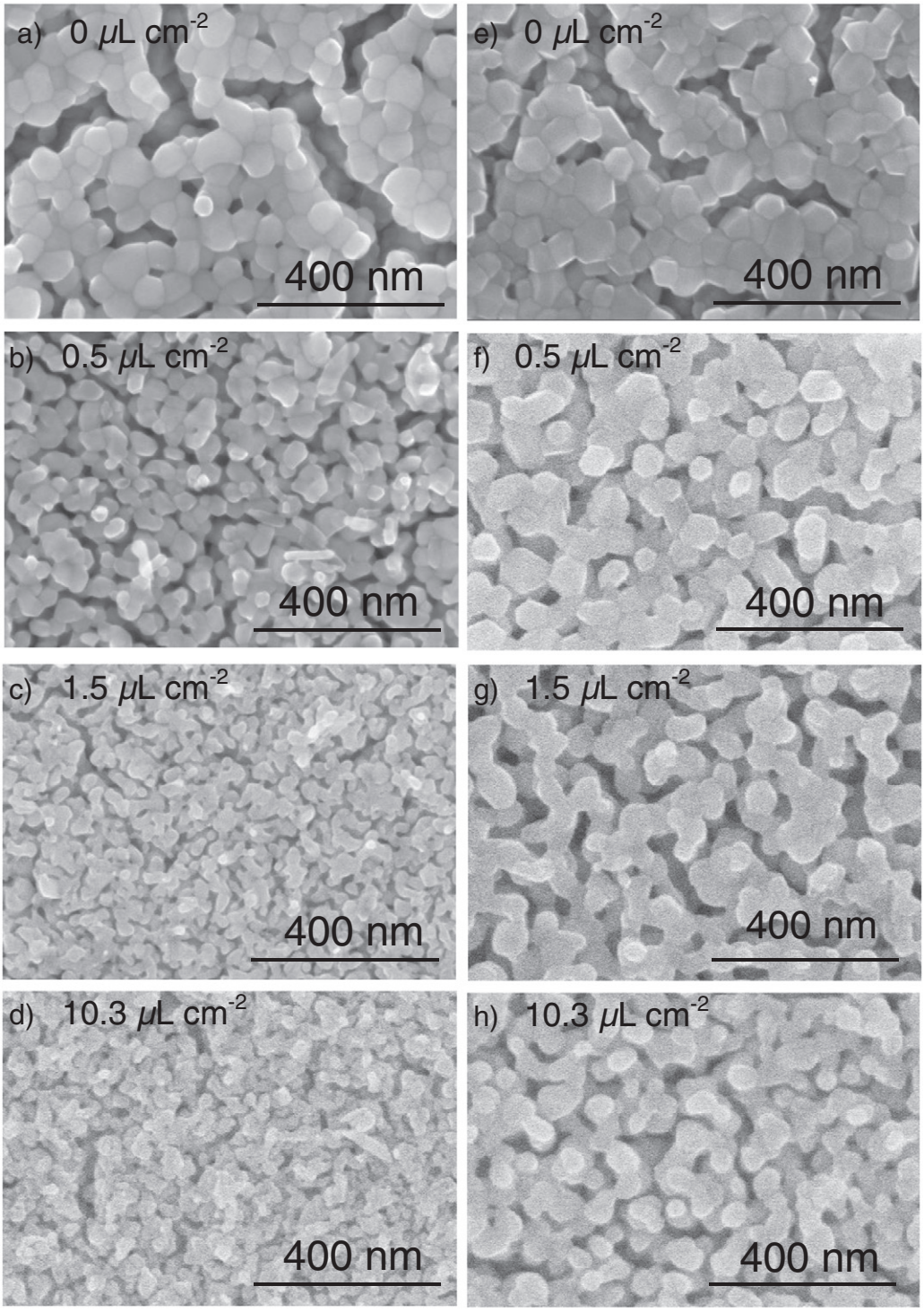

Fig. 2. SEM top views doped with α-Fe_2O_3/FTO electrodes and annealed at 600 °C (a–d) and 600 °C/750 °C (e–h).

magnitude from 0.95 mA cm^{-2} to 1.32 mA cm^{-2}. Also a beneficial shift in the onset potential is observed from 0.9 V (*vs.* RHE) for 0.26 μL cm^{-2} to 0.8 V (*vs.* RHE) for 1.5 μL cm^{-2} dosing.

Following further annealing treatment at 750 °C (Fig. 1c), all electrodes exhibit a strongly enhanced photocurrent. The onset of water oxidation photocurrent for 1.5 μL cm^{-2} Ti dosing is at 0.95 V (*vs.* RHE) reaching 1.4 mA cm^{-2} at 1.23 V (*vs.* RHE), with a maximum photocurrent of 3.1 mA cm^{-2} at 1.8 V (*vs.* RHE). An examination of XPS sputter depth profiles provides the distribution of Sn throughout the iron oxide after annealing at 600 °C and 600 °C/750 °C (Fig. 1d). From TOF-SIMS (inset of Fig. 1d), after annealing at 600 °C a higher Ti concentration at the surface and a tail throughout the sample is present. At 600 °C/750 °C the Ti distribution is homogenized over the sample thickness indicating diffusional penetration. At the same time for 600 °C/750 °C, a Sn concentration-tail throughout the sample is observed. The X-ray diffraction (XRD) patterns for the Ti-free and Ti doped α-Fe_2O_3 electrodes (Fig. 1e) show peaks clearly corresponding to α-Fe_2O_3 (JCPDS 86-0550) on a FTO substrate [22]. In both cases the [110] peak becomes sharper after additional annealing at 750 °C. The strong [110] diffraction implies that the growth axis of the α-Fe_2O_3 nanoparticles is along [110].

It is also interesting to consider the morphology of the structures; Fig. 2 displays micrographs of the different electrodes. The Ti-free α-Fe_2O_3 electrode annealed at 600 °C exhibits a mesoporous structure with round and oval particles of diameters of 40–60 nm (Fig. 2a), whereas the particle diameters are smaller (≈20–40 nm) for Ti doped samples (Fig. 2b–d). One may deduce that decoration with Ti reduces particle aggregation during annealing. A smaller particle size is beneficial due to lower bulk recombination (short life time of excited holes) [3]. Moreover, the overall film porosity increases and provides a larger contact area between semiconductor electrode and electrolyte, which facilitates charge carrier transfer to the electrolyte. The additional annealing at 750 °C (Fig. 2e–h) produces larger feature size of 40–100 nm for the Ti-free sample. The Ti doped electrodes show slightly lower particle sizes but an obviously less sintered morphology compared with the Ti-free electrode.

Fig. 3a shows the incident photocurrent conversion efficiencies (IPCEs) as a function of the incident light wavelength for various amounts of Ti loading on the α-Fe_2O_3 electrodes measured at an applied potential of 1.5 V (*vs.* RHE). Over the entire range from 300 nm to 600 nm, Ti loading leads to an enhanced IPCE compared with

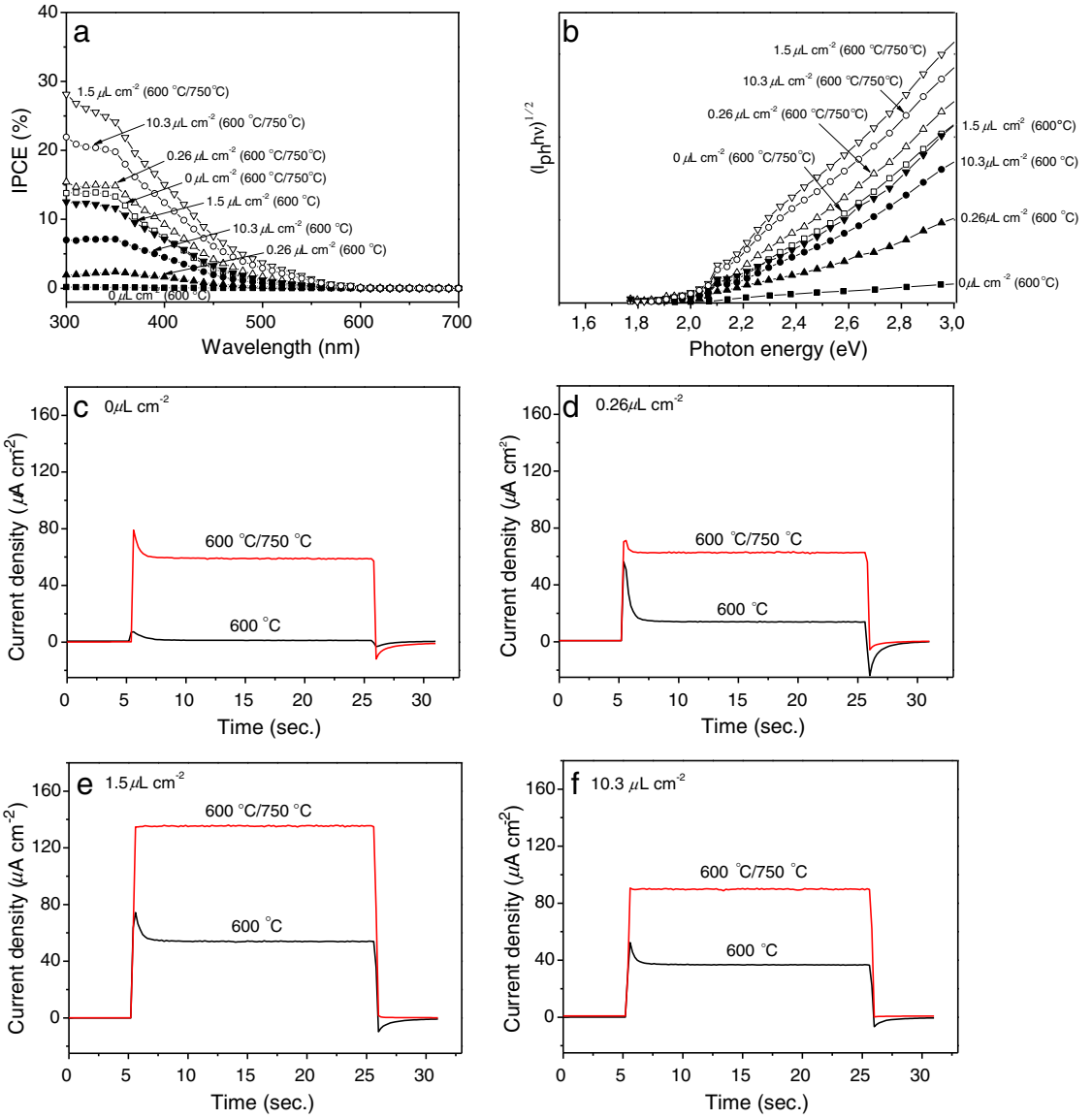

Fig. 3. (a) Incident photon conversion efficiency (IPCE) at an applied potential of 1.5 V (*vs.* RHE) in 1 M KOH for Ti doped α-Fe_2O_3/FTO electrodes annealed at 600 °C and 600 °C/750 °C; (b) the band gap was determined from $(i_{ph}h\upsilon)^{1/2}$ *vs.* photon energy ($h\upsilon$) plots for the corresponding Ti doped α-Fe_2O_3/FTO electrodes; (c–f) photocurrent at 360 nm at an applied potential of 1.5 V (*vs.* RHE) in 1 M KOH for various amounts of Ti (0.2 M $TiCl_4$) doped α-Fe_2O_3 and Ti/Sn co-doped α-Fe_2O_3 electrodes.

the Ti-free electrode, and electrodes annealed at 600 °C/750 °C result in a significantly enhanced IPCE compared with those annealed at 600 °C. The maximum IPCE values are 25% and 12% at 330 nm for 1.5 μL cm^{-2} dosed Ti electrodes annealed at 600 °C/750 °C and 600 °C, respectively. The resulting indirect band-gap E_g values, i.e. from a $(i_{ph}h\upsilon)^{1/2}$ *vs.* photon energy ($h\upsilon$) plot, are in the order of 1.9–2.1 eV (Fig. 3b), in accordance with reported data for α-Fe_2O_3 [4]. The effect of the combined Ti/Sn doping becomes more clearly from the transient photoresponse behavior (Fig. 3c–f). The transient ratio values ($i_{steady}/i_{initial}$) are in the range of 0.25–0.73 after annealing at 600 °C, whereas for Ti doping after annealing at 600 °C/750 °C, the transient ratio values close to one have been attained (except for the Ti-free sample). From the comparison it is evident that doping is particularly effective in reducing/eliminating the decay of the photocurrent (i.e. in combination with Sn doping leads to rectangular phototransients). Even though it is not evidently clear if the main effect of Ti is surface related (e.g. by decorating recombination centers with TiO_2), due to some bulk doping effects, or is morphology related, the present paper clearly shows that doping can aid to strongly suppress charge carrier recombination [23,24].

4. Conclusions

We have demonstrated the feasibility to strongly improve α-Fe_2O_3 electrodes produced by a simple anodic deposition technique by combining a $TiCl_4$ treatment and Sn doping. Results show that the combined process performed in this work leads to a drastically lower recombination rate, which can be ascribed to electronic effects, i.e. substitutional doping and/or surface passivation combined with morphological effects. Optimal Ti doping amount (1.5 μL cm^{-2} of 0.2 M $TiCl_4$) on α-Fe_2O_3 annealed at 600 °C/750 °C reaches remarkable 1.4 mA cm^{-2} at 1.23 V (*vs.* RHE), with a maximum photocurrent of 3.1 mA cm^{-2} at 1.8 V (*vs.* RHE) in 1 M KOH under AM 1.5 (100 mW cm^{-2}) conditions.

Acknowledgments

The authors would like to acknowledge Anja Friedrich, Helga Hildebrand, and Ulrike Marten-Jahns for their assistance in the SEM, XPS, and XRD measurements. We thank DFG and the DFG cluster of excellence “Engineering of Advanced Materials” (EAM) for the financial support.

References

[1] A. Fujishima, K. Honda, Nature 238 (1972) 37.
[2] A. Duret, M. Grätzel, The Journal of Physical Chemistry B 109 (2005) 17184.
[3] J. Brillet, M. Grätzel, K. Sivula, Nano Letters 10 (2010) 4155.
[4] K. Sivula, F. Le Formal, M. Grätzel, ChemSusChem 4 (2011) 432.
[5] S.D. Tilley, M. Cornuz, K. Sivula, M. Grätzel, Angewandte Chemie, International Edition 49 (2010) 6405.
[6] F.J. Morin, Physical Review 83 (1951) 1005.
[7] F.J. Morin, Physical Review 93 (1954) 1195.
[8] Y.Q. Liang, C.S. Enache, R. Van De Krol, International Journal of Photoenergy 2008 (2008) 739864.
[9] I. Cesar, A. Kay, J.A.G. Martinez, M. Grätzel, Journal of the American Chemical Society 128 (2006) 4582.
[10] J.H. Kennedy, M. Anderman, R. Shinar, Journal of the Electrochemical Society 128 (1981) 2371.
[11] N. Uekawa, M. Watanabe, K. Kaneko, F. Mizukami, Journal of the Chemical Society, Faraday Transactions 91 (1995) 2161.
[12] C.J. Sartoretti, M. Ulmann, B.D. Alexander, J. Augustynski, A. Weidenkaff, Chemical Physics Letters 376 (2003) 194.
[13] J.A. Glasscock, P.R.F. Barnes, I.C. Plumb, N. Savvides, Journal of Physical Chemistry C 111 (2007) 16477.
[14] G. Wang, Y. Ling, D.A. Wheeler, K.E.N. George, K. Horsley, C. Heske, J.Z. Zhang, Y. Li, Nano Letters 11 (2011) 3503.
[15] Y.S. Hu, A. Kleiman-Shwarsctein, A.J. Forman, D. Hazen, J.N. Park, E.W. McFarland, Chemistry of Materials 20 (2008) 3803.
[16] H.G. Cha, J. Song, H.S. Kim, W. Shin, K.B. Yoon, Y.S. Kang, Chemical Communications 47 (2011) 2441.
[17] A. Kleiman-Shwarsctein, Y.S. Hu, A.J. Forman, G.D. Stucky, E.W. McFarland, Journal of Physical Chemistry C 112 (2008) 15900.
[18] Y. Ling, G. Wang, D.A. Wheeler, J.Z. Zhang, Y. Li, Nano Letters 11 (2011) 2119.
[19] J.S. Jang, J. Lee, H. Ye, F.R.F. Fan, A.J. Bard, Journal of Physical Chemistry C 113 (2008) 6719.
[20] L. Wang, C.Y. Lee, P. Schmuki, Electrochimica Acta 91 (2013) 307.
[21] L. Wang, C.Y. Lee, P. Schmuki, Journal of Materials Chemistry A 1 (2013) 212.
[22] R.L. Spray, K.S. Choi, Chemistry of Materials 21 (2009) 3701.
[23] S.R. Pendlebury, M. Barroso, A.J. Cowan, K. Sivula, J. Tang, M. Grätzel, D.R. Klug, J.R. Durrant, Chemical Communications 47 (2011) 716.
[24] S.R. Pendlebury, A.J. Cowan, M. Barroso, K. Sivula, J. Ye, M. Grätzel, D.R. Klug, J. Tang, J.R. Durrant, Energy & Environmental Science 5 (2012) 6304.